ACS Chemical Neuroscience pubs.acs.org/acschemicalneuroscience



# Y95 and E444 Interaction Required for High-Affinity S-Citalopram Binding in the Human Serotonin Transporter

Steven Combs,[†] Kristian Kaufmann,[†] Julie R. Field,[‡] Randy D. Blakely,[‡,§,∥] and Jens Meiler*[,†,‡]

[†]Departments of Chemistry, [‡]Pharmacology, and [§]Psychiatry, [∥]Center for Molecular Neuroscience, Vanderbilt University, Nashville, Tennessee, United States

## Abstract

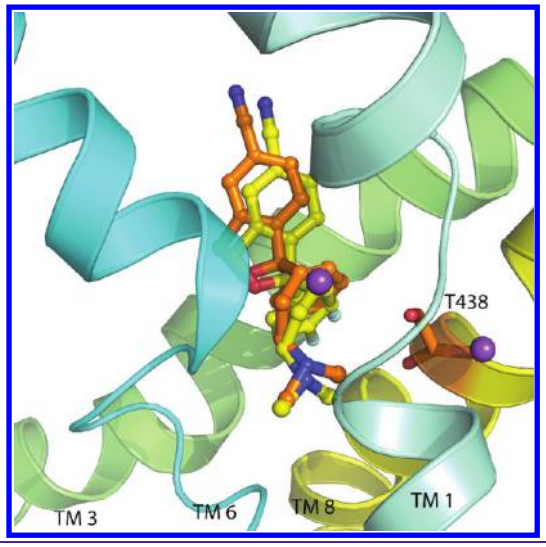


The human serotonin (5-hydroxytryptamine, 5-HT) transporter (hSERT) is responsible for the reuptake of 5-HT following synaptic release, as well as for import of the biogenic amine into several non-5-HT synthesizing cells including platelets. The antidepressant citalopram blocks SERT and thereby inhibits the transport of 5-HT. To identify key residues establishing high-affinity citalopram binding, we have built a comparative model of hSERT and *Drosophila melanogaster* SERT (dSERT) based on the *Aquifex aeolicus* leucine transporter ($LeuT_{Aa}$) crystal structure. In this study, citalopram has been docked into the homology model of hSERT and dSERT using RosettaLigand. Our models reproduce the differential binding affinities for the *R*- and *S*-isomers of citalopram in hSERT and the impact of several hSERT mutants. Species-selective binding affinities for hSERT and dSERT also can be reproduced. Interestingly, the model predicts a hydrogen bond between E444 in transmembrane domain 8 (TM8) and Y95 in TM1 that places Y95 in a downward position, thereby removing Y95 from a direct interaction with *S*-citalopram. Mutation of E444D results in a 10-fold reduced binding affinity for *S*-citalopram, supporting the hypothesis that Y95 and E444 form a stabilizing interaction in the *S*-citalopram/hSERT complex.

**Keywords:** *S*-citalopram, hSERT, ligand, homology model, computational docking

Depression affects close to 121 million people world wide (*2*). The monoamine theory postulates that disruption or malfunction of CNS serotonergic and noradrenergic systems drives the risk and/or symptoms of depression (*3*). The human 5-HT transporter (hSERT, *SLC6A4*) is an integral membrane protein localized to serotonergic terminals. SERT is responsible for the uptake of 5-HT, $Na^+$ ions, and $Cl^-$ ions across the presynaptic cell membrane, thereby limiting 5-HT actions in space and time (*4*). A variety of brain disorders, including depression, are linked to alterations in uptake of 5-HT from the presynaptic cell membrane via hSERT (*5*). For treatment of depression, selective 5-HT reuptake inhibitors (SSRIs) were developed that elevate 5-HT levels at the synapse. One such SSRI, citalopram, alleviates the symptoms of depression and is the focus of our current study (*6*).

The stereochemistry of citalopram determines its activity. The active *S*-configuration binds with high-affinity to hSERT, whereas the *R*-configuration exhibits reduced binding affinity at hSERT but may also modulate interactions of the *S*-isomer with the transporter (*7*). Although the effects of citalopram are well studied, the structural determinants of interactions of *S*- and *R*-citalopram with hSERT remain a focus of current investigations. We have shown that *S*- and *R*-citalopram exhibit potency differences between hSERT and dSERT that largely derive from interactions with two residues (Y95 and I172 in hSERT) (*7*). These differences provide an important, suitable test of small molecule docking methods to homology models of SERT proteins, an approach we have recently used for the docking of 5-HT (*8*). Here, we dock both stereoisomers of citalopram computationally into models of

**Received Date:** July 16, 2010
**Accepted Date:** October 11, 2010
**Published on Web Date:** October 27, 2010





DOI: 10.1021/cn100066p | *ACS Chem. Neurosci.* (2011), *2*, 75–81

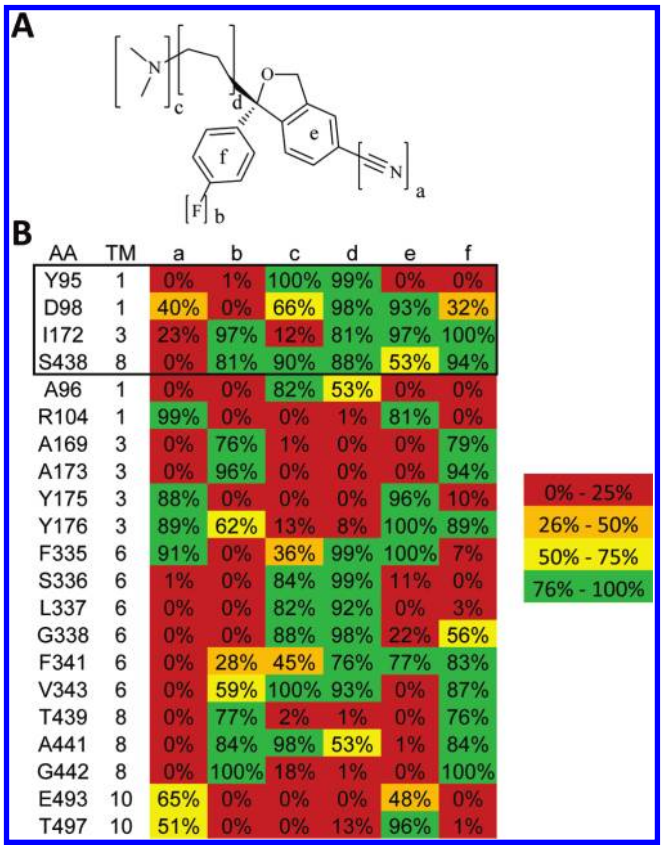


**Figure 1.** (A) *S*-Citalopram functional groups involved in binding are labeled a−f. (B) Contacts within the *S*-citalopram/hSERT high-affinity binding mode are displayed as a heatmap. Given is the fraction of models that display a contact within the largest cluster of models. Residues known to affect *S*-citalopram binding are shown within the black box.

human and fly SERT. The predictive power of the models is tested by introducing known mutations that disrupt *S*- and *R*-citalopram interactions with hSERT. Our models recapitulate the species-selective binding affinity differences between hSERT and *Drosphila* SERT (dSERT), as well as the distinct binding affinities of *S*- and *R*-citalopram isomers to wild type transporters.

SERT homology models were constructed on the basis of multiple sequence alignments (*9*) of SLC6 family members with the crystal structure of $LeuT_{Aa}$ as a template (*10*). A series of structure−activity relationships (SAR) and mutational studies guide the analysis of structural determinants of *S*-citalopram binding (Figure 1A). The cyano group [a], the dimethyl-amine [c], and the fluorine of the flouro-phenyl substituted ring [b] of *S*-citalopram were determined as key functional groups for inhibitor potency through substitution with hydrogen (*11*). Through mutational studies, several amino acids have been identified as dictating high affinity binding for *S*-citalopram. D98 is known as a conserved residue found in all monoamine transporters and has been shown to stabilize a protein−ligand salt bridge (*12*). Henry et al. (*7*) produced point mutations to convert two residues in hSERT to the corresponding dSERT residues (Y95F and I172M), resulting together in a ~6,000-fold loss of potency for *S*-citalopram (*7*). The single mutations of Y95F and I172M resulted in a 19- and 344-fold loss, respectively. In contrast, *R*-citalopram displays a 79- and 5-fold loss of potency for the same mutations and only a 117-fold loss if the mutations are combined. In this study, we propose that the dimethyl-amine group [c] of *S*-citalopram interacts with Y95, while the cyanophthalane ring [e] and the flouro-phenyl ring [f] interact with I172 (*7*). More recently, Andersen et al. (*13*) have demonstrated the importance of S438 in binding the dimethyl-amine group [c] through a mutation S438T that results in a 300-fold loss of potency for *S*-citalopram; however, the S438T mutant only results in a loss of potency of 15−20-fold for *R*-citalopram (Andersen, J., personal communication).

Site-directed mutagenesis of hSERT and dSERT in pcDNA3.1 was performed using the QuikChange mutagenesis kit and protocol (Stratagene). Sense and antisense oligonucleotides, purchased from Invitrogen, were designed to generate the single amino acid substitutions. Oligonucleotide sequences used for mutagenesis are available upon request. Sequencing of all mutants was performed at the DNA Sequencing Facility of the Division of Genetic Medicine at Vanderbilt University Medical Center. Successful mutants were transformed into DH5α *Escherichia coli* cells for amplification and purified using the Qiafilter Maxiprep kit (Qiagen). HEK-293 cells, maintained at 37 °C in a 5% $CO_2$ humidified incubator, were grown in complete medium (Dulbecco's modified Eagle' medium, 10% fetal bovine serum, 2 mm L-glutamine, 100 units/mL penicillin, and 100 μg/mL streptomycin). For initial evaluation of mutant transporter activity, cells were plated at a density of 50,000 cells per well in 24-well culture plates. Cells were transfected with hSERT or dSERT constructs using TransIT transfection reagent (Mirus Inc., 6 μL per μg of DNA), in Opti-MEM medium. Following transfection (24−48 h), cells were washed with KRH assay buffer (120 mM NaCl, 4.7 mM KCl, 2.2 mM $CaCl_2$, 1.2 mM $MgSO_4$, 1.2 mM $KH_2PO_4$, and 10 mM HEPES, pH 7.4) and incubated for 10 min with increasing concentrations of nonradiolabeled competitor, followed by the addition of a constant concentration of [$^3$H]5-HT (5-hydroxy[$^3$H]tryptamine-trifluoroacetate (100−110 Ci/mmol); Amersham Biosciences) for 15 min. Transport assays were terminated by washing two times with assay buffer, and cells were dissolved in MicroScint 20 (PerkinElmer Life Sciences) scintillation fluid. The extent of [$^3$H]5-HT accumulation was determined by liquid scintillation counting on a TopCount System (PerkinElmer Life Sciences). Uptake in



DOI: 10.1021/cn100066p | *ACS Chem. Neurosci.* (2011), *2*, 75–81

mock-transfected cells was subtracted from transporter-transfected cells to determine specific uptake. Specific uptake was normalized to the percent uptake of control wells that lacked the competitor and plotted versus the log of the molar concentration of competitor. The data were fit to a nonlinear one-site competition curve, and apparent $K_i$ values were derived using the Cheng−Prusoff equation in Prism 4 for Macintosh (Graphpad Software). All experiments were performed in triplicate and repeated in three or more separate assays.

RosettaLigand (*14*) was used to dock *S*- and *R*-citalopram separately into the hSERT homology models while accounting for full protein and ligand flexibility. Specifically, the protein backbone conformation underwent repeated energy minimization from the initial homology model which resulted in a large conformational ensemble of backbones. An ensemble of the top 10 energy minimized backbones was used in the docking steps. Amino acid side chain conformations were chosen from a rotamer library (*15*) and further optimized through gradient minimization. Ligand flexibility was modeled through knowledge-based torsion angle potentials derived from the chemical Cambridge Structural Database (CSD) (*16*) yielding a total of 1,000 *S*- and *R*-citalopram conformations. The generation of 1,000 conformations for *S*- and *R*-citalopram allows for thorough sampling of nonclashing conformations for the five rotatable bonds. The generation of 1,000 conformations for *S*- and *R*-citalopram allows for thorough sampling of non-clashing conformations for the five rotatable bonds. The 1,000 conformations cluster into 238 distinct rotamers and allows for an average of three states for each of the five bonds to be independently sampled. The protocol for the construction of these homology models, the creation of conformational ensembles, and docking are described in detail elsewhere (*8*). A total of 23,500 models for the *S*-citalopram/hSERT and *R*-citalopram/hSERT complex were created.

Our models were first filtered according to their RosettaLigand binding energy selecting the top 10%. The resulting 2,350 models were clustered into separate binding modes based upon a 3.0 Å rmsd threshold. This resulted in multiple clusters of varying size. The models presented here are the lowest energy models from the largest clusters, respectively. After a binding mode had been established for *S*-citalopram/hSERT and *R*-citalopram/hSERT complexes, mutations were introduced into the hSERT backbone while maintaining the putative binding mode of the *S*-citalopram/hSERT and *R*-citalopram/hSERT complexes. The mutations analyzed were Y95F, I172M, S438T, and the double mutant Y95F/I172M. After introduction of the mutations, each model was refined through Monte Carlo moves of up to 2.0 Å and 10.0° for the ligand, while the protein backbone and side-chains were minimized. For each mutant, the models with the lowest RosettaLigand binding energy were analyzed. To explore the proposed conformation of *S*-citalopram in relation to dSERT, the putative binding mode of the *S*-citalopram/hSERT complex was placed into nine different backbones of dSERT (*16*). The binding mode underwent Monte Carlo refinement and optimization. The lowest energy was chosen for analysis.

A single cluster of interactions for the *S*-citalopram/hSERT complex stood out by both its size (400 members out of a total of 2,350 models) and RosettaLigand binding energy of −8.1 Rosetta Energy Unit (REU) (Figure 2A). This model preserves the hypothesized D98 (*12*) dimethyl-amine [c] contact along with a hydrogen bond between the dimethyl-amine group [c] and the backbone carbonyl group of Y95 (*7*). Additionally, the dimethyl-amine group [c] is in contact with S438. The model is further characterized by a hydrophobic clamp that is formed by the flouro-phenyl ring [f] and the cyanophthalane ring [e] around I172 (*7*).

*S*-Citalopram/hSERT contacts were compiled as a heat map to illustrate amino acid residues in and around the *S*-citalopram binding pocket of our model (Figure 1B). Novel contacts proposed by the present model include the methylene groups of the 3-(dimethylamino)propyl tail [d] which form van der Waals (VDW) contacts with residues S336, L337, and G338 in TM 6 and A441 in TM 8. The cyano group [a] is pointed toward the extracellular space, out of the membrane and binding pocket, and toward residue R104 in TM 1 and E494 in TM 10, and has VDW contacts with G100 in TM 1, F335 in TM 6, and Y175 and Y176 in TM 3. Additionally, the flouro-phenyl ring [f] sits in a hydrophobic pocket created by residue A169 (*17*) in TM 1 and A441 and G442 in TM 8.

Docking of *R*-citalopram results in two clusters of similar size and energy. The largest cluster (124 members out of 2,350) has an energy of −6.5 REU and is in a different conformation found in the *S*-citalopram/hSERT complex. Interestingly, the second largest cluster has *R*-citalopram in a conformation similar to that of the *S*-citalopram/hSERT complex; however, the dimethyl-amine tail [c] is distant from S438 and pointed in the direction between TM 1 and TM 6. To remain consistent with the analysis of *S*-citalopram, analysis of the largest cluster was performed for *R*-citalopram.

Our model indicates that the *R*-citalopram/hSERT complex has a significantly different binding conformation than the *S*-citalopram/hSERT complex. The cyanopthalane ring [e] and dimethyl-amine [c] of *R*-citalopram are shifted out of the binding pocket and positioned toward the extracellular face of the transporter. In particular, R104 in TM 1 and E493 in TM 10 form hydrogen bonds with the dimethyl-amine group [c],



DOI: 10.1021/cn100066p | *ACS Chem. Neurosci.* (2011), *2*, 75–81

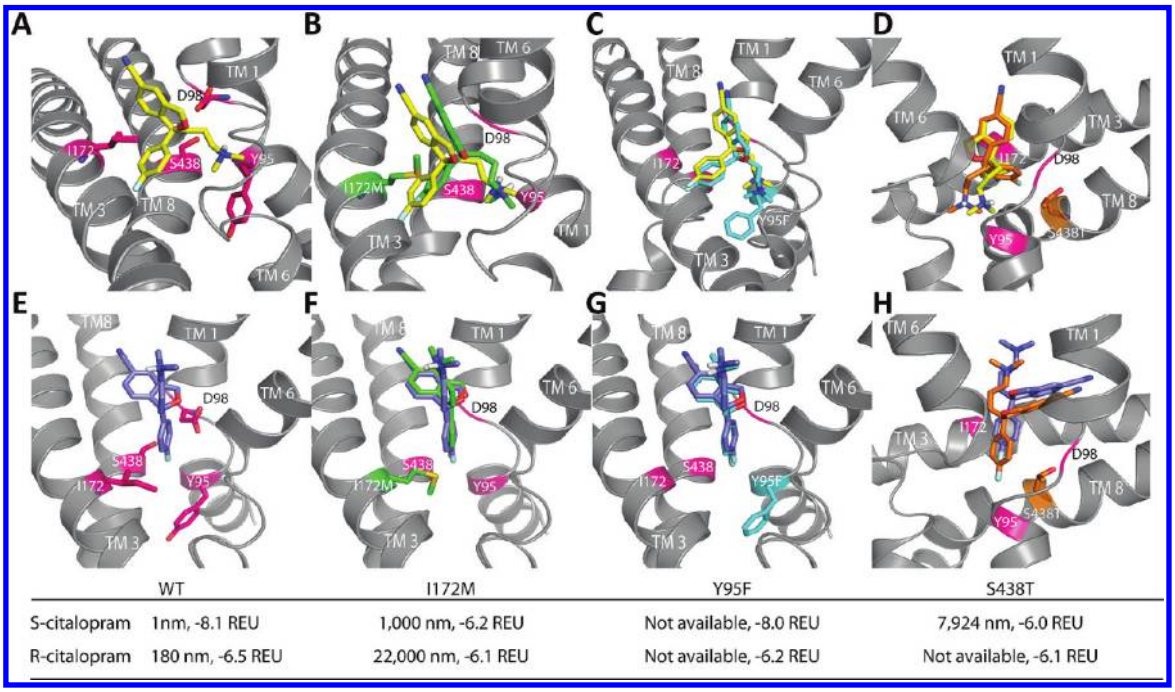


**Figure 2.** *S*- and *R*-citalopram in complex with mutants of hSERT. The extracellular side of the protein is shown on the top of all images, whereas the cytoplasm is at the bottom of all images. The *S*-citalopram/hSERT complex is shown on top, and the *R*-citalopram/hSERT complex is shown below. Experimental binding affinities, $K_i$, and computationally predicted binding energies are given below each image. (A and E) WT hSERT in complex with *S*- and *R*-citalopram. Experimentally verified residues involved in binding are shown as sticks and highlighted in red and labeled. (B and F) *S*- and *R*-citalopram putative wild type binding mode docked into the I172M mutant of hSERT (green). The original wild type binding mode is displayed in yellow and blue (*S*-citalopram and *R*-citalopram, respectively). The mutation I172M is shown in green and stick format with the experimentally verified residues shown in cartoon and highlighted with red. (C and G) *S*- and *R*-citalopram docked into the Y95F mutant. The putative wild type binding is colored cyan with the mutant Y95F colored in cyan and shown as a stick. (D and H) *S*- and *R*-citalopram docked into S438T. The putative wild type binding is colored in orange with the mutant S438T shown in sticks and colored orange.

whereas the cyano group [a] is directed toward W103 in TM 1. The flouro-phenyl ring [f] sits in the binding pocket and is pointed downward toward Y95 and D98 in TM 1. Additionally, Y175 in TM 3 is $\pi$ -stacked against the flouro-phenyl fing [f].

To test our models, the putative binding modes for *S*- and *R*-citalopram were examined via *in silico* mutations that have been previously studied experimentally: I172M, Y95F, S438T, and an I172M/Y95F double mutant (*7*, *13*). Experimentally, the I172M mutation results in a 344-fold loss of potency for *S*-citalopram (*7*). Accordingly, docking into the I172M mutant results in a reduced binding energy of −6.2 REU (Figure 2). The conformation of *S*-citalopram within the binding pocket is shifted away from the site of mutation, I172M. The reduction in score is attributed to compromised hydrophobic packing at site 172 and loss of a $\pi$-stacking interaction with F355.

Experimentally, *S*-citalopram interaction with a Y95F mutant of hSERT results in a 19-fold loss of potency (*7*). This experimental finding as well as studies with 5-HT suggest that Y95 is directly involved in hSERT interaction with ligands (*7*). However, our comparative model has Y95 pointing away from the binding pocket and engaged in a hydrogen bond with E444. A conformational change of Y95 into an upward pointing conformation requires substantial rearrangement of the protein backbone from the template structure $LeuT_{Aa}$ and breaking of the Y95-E444 hydrogen bond. To experimentally test the effects of breaking the hypothesized Y95-E444 hydrogen bond with minimal impact on other areas of the transporter, an hSERT E444D mutant was created. We found that this mutant displays a modest, 10-fold loss of potency for *S*-citalopram (Figure 3A,B). This observation supports the contention that E444 is indirectly involved in citalopram binding. Our data does not conclusively prove that E444 locks Y95 into a downward orientation required for high-affinity binding of citalopram. We speculate that an upward pointing conformation of Y95 may be engaged in earlier stages of *S*-citalopram binding (e.g., an outward facing, open conformation of hSERT) followed by the downward pointing conformation by binding of *S*-citalopram, thereby explaining the experimental findings (Figure 3). Regardless, docking studies of *S*-citalopram/Y95F hSERT resulted in a slightly reduced binding energy of −8.0 REU coupled with a shift of *S*-citalopram away from the extracellular face



DOI: 10.1021/cn100066p | *ACS Chem. Neurosci.* (2011), *2*, 75–81

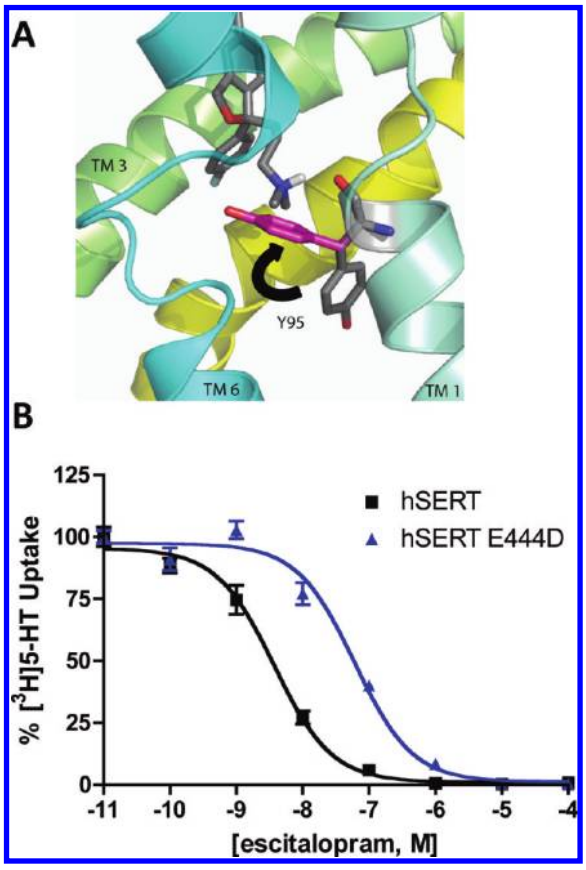


**Figure 3.** (A) Binding mode of the *S*-citalopram/hSERT complex with the depiction of the Y95 (gray) in a downward position. Mutation of E444D (not shown) results in Y95 populated in two positions, a downward position (gray) and an upward position (pink). (B) Mutation of E444D results in a 10-fold loss of potency for *S*-citalopram suggesting that the Y95 switches between two different conformations: upward (pink) and downward conformations (gray). The wild type is shown in by black squares and a line, and E444D is shown in circles and spheres.

of hSERT to deeper inside the binding pocket toward F95.

Similar to the I172M mutation, our model of the Y95F/I172M double mutant predicts a movement of *S*-citalopram away from I172M and a reduced binding energy of −7.6 REU. The loss in binding affinity is largely attributed to the I172M mutation.

Recently, Andersen (*13*) and colleagues mutated S438T and tested the mutant against the binding of dimethylated inhibitors. A mutation of S438T resulted in a loss of potency for dimethylated inhibitors; however, a 300-fold loss for *S*-citalopram potency was reported. In our model, the *S*-citalopram complex with the S438T mutant results in a significant reduction of energy to −6.0 REU. The dimethyl-amine group [c] shifts away from T438, which results in repulsive interaction with residues on TM 1. The influence of $Na^+$ ions on the S438T mutant was also tested. However, no significant change in the model and energy was observed (see Supporting Information).

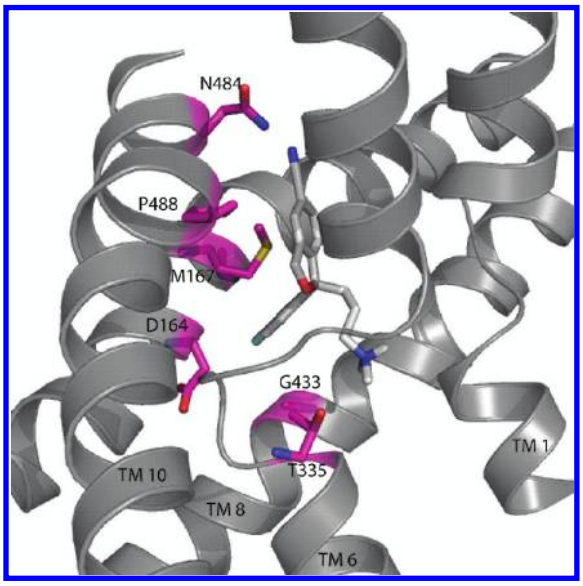


**Figure 4.** Putative binding mode of the *S*-citalopram/dSERT complex. *S*-Citalopram is shown in white. Residues that contribute to lowering the energy of the complex are highlighted in red. Substitution of A169 to D164 dSERT results in a higher solvation score for the complex. Additionally, M167 dSERT results in an increase in the VDW potential.

For *R*-citalopram, the introduction of bulk via the I172M mutation results in a slight loss of binding energy to −6.1 REU, in agreement with experimental findings (*7*). The flouro-phenyl ring [f] is shifted away from the mutation and toward TM 1 and TM 6. The Y95F hSERT mutation results in a slightly lower binding energy than that of the wild type (−6.2 REU). The double mutant I172M/Y95F (−6.1 REU) displays an additional shift of the flouro-phenyl ring [f] away from M172, consistent with the contention that I172 is a critical contact site for the SSRI (*7*). Andersen reported that a mutation of S438T resulted in a 15-fold loss of potency for the *R*-citalopram/hSERT complex (personal communication). In agreement with his findings, the *R*-citalopram/S438T hSERT complex displays a reduced binding energy of −6.1 REU coupled with a shift away from the site of mutation.

To further validate the *S*-citalopram/hSERT model, dSERT homology models were used to dock the putative binding mode of *S*-citalopram. dSERT differs in selectivity for racemic citalopram compared to that of hSERT. Racemic citalopram exhibits a $K_i$ value of 400 nM in dSERT (*12*); however, a point mutation of M167I (I172 hSERT) results in an increase of binding affinity to 4 nm (*7*). To determine if our docking paradigm could reproduce the experimental finding, *S*-citalopram/dSERT models were constructed. The *S*-citalopram/dSERT binding energy for the lowest-energy pose (Figure 4) was significantly worse when compared to that of the *S*-citalopram/hSERT complex



DOI: 10.1021/cn100066p | *ACS Chem. Neurosci.* (2011), *2*, 75–81

(−6.6 REU and −8.1 REU, respectively). This loss is attributed to two energy contributions when comparing the two models, the hydrogen bonding term and the solvation term (+0.8 REU and +0.7 REU, respectively). Specifically, a network of hydrogen bonding interactions between side-chains and the cyano group [a] in *S*-citalopram/hSERT are absent in the *S*-citalopram/dSERT model. The hSERT residues that are hydrogen bonded to the cyano group [a] are R104 and E493. Although R104 is preserved in dSERT, E493 is substituted to N, which is predicted to alter the hydrogen bond network. To test the significance of the hydrogen bond network, reciprocal mutants of hSERT E493N and dSERT N481E were constructed and tested for *S*-citalopram potency. We observed an ∼3-fold average loss of potency in the hSERT E493N mutant that did not reach statistical significance (data not shown). The reciprocal mutation dSERT N481E was without effect. We had hypothesized that the E493-R104 salt-bridge in hSERT positions R104 for a constructive interaction with the cyano group [a]. Therefore, a N481E mutation in dSERT was expected to increase *S*-citalopram affinity. However, the interaction between R99 (residue R104 in hSERT) and the cyano group [a] in wild type dSERT is not strengthened through the N481E mutation. A possible explanation is that the positive charge of R104 is compensated through E481 weakening the interaction with the partial negative charge of the cyano group [a]. Additional experiments are needed to verify this hypothesis.

The change of solvation energy of *S*-citalopram in our models can be attributed to the burial of the flouro-phenyl ring [f] in a hydrophobic environment. hSERT and dSERT residues are homologous in this region, with the exception of hSERT residues A169 and I172 which correspond to dSERT residues D164 and M167. Of these two residues, the solvation energy for hSERT A169 and dSERT D164 are drastically different (+1.1 REU in dSERT). This finding matches experimental studies that affiliate the A169D point mutation with a loss of *S*-citalopram potency in hSERT (*17*). Furthermore, the I172M mutation in hSERT causes a binding energy increase in the VDW potential of the *S*-citalopram/hSERT complex by +2.8 REU. As discussed above, the hSERT I172M mutant has been tested experimentally and displayed a significant loss of *S*-citalopram potency. However, when the reverse mutant is expressed, dSERT M167I, dSERT regains hSERT-like potency for *S*-citalopram (*7*). When the computational mutant is tested, an energy similar to that of *S*-citalopram/hSERT is observed. *S*-Citalopram/dSERT M167I results in an energy of −8.1 REU and recapitulates the docked *S*-citalopram/hSERT pose.

Recently, Andersen et al. (*18*) published an independent computational model for *S*-citalopram in hSERT. The authors created 64 point mutants to validate their binding mode. The proposed model by Andersen et al. places the cyano group [a] sandwiched between TM 6 and 8, whereas our model positions the cyano group [a] outward toward the extracellular face of the protein. This results in a 5.1 Å rmsd in ligand placement compared to our model. The ligand occupies the same binding pocket but experiences a ∼30° rotation. A qualitative and quantitative comparison of mutation data presented by Andersen et al. displays a similar level of agreement between the two models suggesting that further experiments are needed to more precisely define the position of *S*-citalopram (see Supporting Information). One noticeable difference between the models and reason for the slight shift and rotation in the *S*-citalopram is a manual positioning of the Y95 residue in an upward configuration, providing new contacts with *S*-citalopram. Experiments are needed to validate this positioning of Y95 during the transport cycle and antagonist binding. They also identify unexpected interactions between TM 1 and 8 that may contribute to critical conformational transitions in the dynamic organization of other SLC6 transporters.

In addition to Andersen's model, Koldsø et al. (*19*) created models of *S*-citalopram and *R*-citalopram complexed in hSERT. Unfortunately, the coordinates of these models are not available to us for quantitative comparison. Qualitatively, the *S*-citalopram/hSERT complex proposed compares to the model presented here. In Koldsø's model, the flouro-phenyl ring [f] is in the hydrophilic pocket lined by A169, A173, N177, S438, T439, and L443. Our model positions the flouro-phenyl ring [f] in this pocket as well. The cyano group [a] in Koldsø's model is positioned next to T497, F335, F341, and V501. In contrast, our model positions the cyano group [a] pointed outside of the binding pocket and is next to F335, R104, and E493.

The *R*-citalopram conformations are noticeably different. Koldsø's *R*-citalopram/hSERT complex differs from the *S*-citalopram/hSERT complex by the reverse placement of the cyanophthalane ring [e] and flouro-phenyl ring [f]. In contrast, the presented *R*-citalopram/hSERT in this letter is bound higher in the binding pocket in a completely different conformation. The contrasting results might suggest multiple low affinity binding sites for *R*-citalopram and require further experimental investigation.

In summary, our study confirms aspects of the *S*-citalopram binding mode using orthogonal computational techniques, providing a detailed analysis of the impact of citalopram isomerization and further elucidates the species selectivity for SSRI recognition.

## Supporting Information Available

RosettaLigand command line options as well as *S*-citalopram/hSERT S438T with $Na^+$ ions and quantitative analysis of



DOI: 10.1021/cn100066p | *ACS Chem. Neurosci.* (2011), *2*, 75–81

Anderson's model with mutations and models of *S*-citalopram/hSERT and *R*-citalopram/hSERT. This material is available free of charge via the Internet at http://pubs.acs.org.

## Acknowledgment

We thank Dr. Jacob Andersen for providing us with models and experimental results.

## Author Information

**Corresponding Author**

* Department of Chemistry, Vanderbilt University, VU Station B #351822, 7330 Stevenson Center, Nashville, TN 37235-1822. E-mail: jens.meiler@vanderbilt.edu.

**Funding Sources**

This work was supported by T32 GM 08320 (S.C.), R01 GM 080403 (J.M.), Forest Research Institute (J.M. and R.D.B.), and R01 DA07390 (R.D.B.).

## References

1. Kessler, R. C., Chiu, W. T., Demler, O., Merikangas, K. R., and Walters, E. E. (2005) *Arch. Gen. Psychiatry 62*, 617–627.

2. http://www.who.int/mental_health/management/depression/definition/en/

3. Hirschfeld, R. M. (2000) *J. Clin. Psychiatry. 61* (Suppl. 6), 4–6.

4. Barker, E. L., Burris, K. D., and Sanders-Bush, E. (1991) *Brain Res. 552*, 330–332.

5. Blakely, R. D., Berson, H. E., Fremeau, R. T.Jr., Caron, M. G., Peek, M. M., Prince, H. K., and Bradley, C. C. (1991) *Nature 354*, 66–70.

6. Hyttel, J. (1994) *Int. Clin. Psychopharmacol. 9* (Suppl. 1), 19–26.

7. Henry, L. K., Field, J. R., Adkins, E. M., Parnas, M. L., Vaughan, R. A., Zou, M. F., Newman, A. H., and Blakely, R. D. (2006) *J. Biol. Chem. 281*, 2012–2023.

8. Kaufmann, K. W., Dawson, E. S., Henry, L. K., Field, J. R., Blakely, R. D., and Meiler, J. (2009) *Proteins 74*, 630–642.

9. Beuming, T., Shi, L., Javitch, J. A., and Weinstein, H. (2006) *Mol. Pharmacol. 70*, 1630–1642.

10. Singh, S. K., Yamashita, A., and Gouaux, E. (2007) *Nature 448*, 952–956.

11. Eildal, J. N., Andersen, J., Kristensen, A. S., Jorgensen, A. M., Bang-Andersen, B., Jorgensen, M., and Stromgaard, K. (2008) *J. Med. Chem. 51*, 3045–3048.

12. Barker, E. L., Moore, K. R., Rakhshan, F., and Blakely, R. D. (1999) *J. Neurosci. 19*, 4705–4717.

13. Andersen, J., Taboureau, O., Hansen, K. B., Olsen, L., Egebjerg, J., Stromgaard, K., and Kristensen, A. S. (2009) *J. Biol. Chem. 284*, 10276–10284.

14. Davis, I. W., and Baker, D. (2009) *J. Mol. Biol. 385*, 381–392.

15. Dunbrack, R. L.Jr. (2002) *Curr. Opin. Struct. Biol. 12*, 431–440.

16. Kaufmann, K., Glab, K., Mueller, R., and Meiler, J. (2008) Small Molecule Rotamers Enable Simultaneous Optimization of Small Molecule and Protein Degrees of Freedom in ROSETTA-LIGAND Docking, In *German Conference on Bioinformatics* (Beyer, A., and Schroeder, M., Eds.), pp 148−157, Dresden.

17. Larsen, M. B., Elfving, B., and Wiborg, O. (2004) *J. Biol. Chem. 279*, 42147–42156.

18. Andersen, J.; Olsen, L.; Hansen, K. B.; Taboureau, O.; Jorgensen, F. S.; Jorgensen, A. M.; Bang-Andersen, B.; Egebjerg, J.; Stromgaard, K.; Kristensen, A. S. (2009) *J. Biol. Chem.*

19. Koldso, H.; Severinsen, K.; Tran, T. T.; Celik, L.; Jensen, H. H.; Wiborg, O.; Schiott, B.; Sinning, S. (2010) *J. Am. Chem. Soc., 132*, 1311−1322.

## Note Added after ASAP Publication

This paper was published on the Web on October 27, 2010. The Supporting Information file was revised and the corrected version was reposted on November 18, 2010.





DOI: 10.1021/cn100066p | *ACS Chem. Neurosci.* (2011), *2*, 75–81